A comparative study on the removal of lead from industrial wastewater by adsorption onto raw and modified Iranian Bentonite (from Isfahan area)

Bahareh Sadeghalvad [a] , Hossein. Sh. Karimi [a] , Hamed Hosseinzadegan [a] & Amir Reza Azadmehr [a]

[a] Department of Mining and Metallurgical Engineering , Amirkabir University of Technology , 424 Hafez Avenue, 1875-4413, Tehran , Iran Phone: Tel. +98 91 2419 5819
Published online: 01 Aug 2013.

PLEASE SCROLL DOWN FOR ARTICLE

A comparative study on the removal of lead from industrial wastewater by adsorption onto raw and modified Iranian Bentonite (from Isfahan area)

Bahareh Sadeghalvad, Hossein. Sh. Karimi, Hamed Hosseinzadegan, Amir Reza Azadmehr*

Department of Mining and Metallurgical Engineering, Amirkabir University of Technology, 424 Hafez Avenue, 1875-4413, Tehran, Iran
Tel. +98 91 2419 5819; email: a_azadmehr@aut.ac.ir

ABSTRACT

In recent years, Bentonite has attracted a lot of interest due to its potential applications and capability for removing heavy metals from aqueous solutions. This ability related to the high ionic exchange capacity and specific surface area. In this study, Iranian Bentonite obtained from Isfahan area was characterized by using X-ray diffraction, X-ray fluorescence, and IR spectroscopy. The effects of different parameters have been investigated on the adsorption of lead from aqueous solution such as contact time, metal concentrations, pH of solution, stirring speed, particle size, amount of Bentonite, and solid in comparison with liquid solution. Bentonite has been modified by $NaCl$ and NH_4Cl. As the equilibrium study and the Langmuir, Freundlich, Temkin, and Dubinin–Radushkevich (D–R) models have been used and examined. The correlation coefficients (r^2) of lead adsorption have been increased by modification of Bentonite for all models. In addition, the Langmuir model is the best one with correlation coefficient (r^2) more than 0.995 for description/adsorption process of lead, which is applied on raw Bentonite and modified Bentonite. The correspondence of Langmuir model for maximum adsorption capacity of raw Bentonite, $NaCl$–Bentonite, and NH_4Cl–Bentonite is 79.3, 102.0, and 94.3 mg/g, respectively.

Keywords: Bentonite; Lead; Adsorption; Modification; Adsorption isotherms

1. Introduction

Releasing of lead into the environment has detrimental effects on health. Unfortunately, there is a high risk of undesirable exposure and spread of this pollutant in the environment. It could be discharged into air, water, and soil by many industrial activities such as mining operation, manufacture of storage batteries, painting pigments, petroleum refining, automobiles, and cable covering. Toxicity of lead can cause various health conditions and diseases such as hypertension, nephritis, abdominal pain, constipation, cramps, nausea, vomiting, behavioral changes, learning disabilities, and cancers [1–3]. These diseases caused by lead can be interfered in biological processes which are related to interaction of lead with functional groups of biological molecules.

*Corresponding author.

There are many methods for removing heavy metals from aqueous solution such as ion exchange, solvent extraction, reverse osmosis, chemical precipitation, adsorption, and membrane processes [4–6]. The adsorption method is one of the popular methods for removing of heavy metal from solution, which has been performed by two categories of synthesized and natural materials. The synthesized materials are active carbon [7], magnetic [8], zeolite [9], and natural minerals which contain mineral material, industrial, agricultural, and forest wastes. However, natural minerals such as Bentonite [10], Kolanite [11], and Zeolite [12] are widely applied in many fields of technology and science for removing heavy metals and organic pollutants from solution and gas.

Bentonite is volcanic clay. Montmorillonite is the main clay mineral constituent of Bentonite and belongs to Smectitic clay minerals with $(Na, Ca)_{0.33}$ $(Al, Mg)_2Si_4O_{10}(OH)_2 \cdot nH_2O$ formula. Montmorillonite has layer structure with one octahedral coordinated layer of aluminum as the basic structural unit, which is sandwiched between two tetrahedral coordinated layers of silicon. The electrostatic interaction between these layers is a weak Van Der Waals force, which facilitates intercalation process. Net negative surface charge on the Bentonite due to the defect of crystal frame work that has been originated substitution of aluminum ion for silicon ion and magnesium or iron ions for aluminum in the tetrahedral sheets and octahedral sheets, respectively. The exchangeable cations such as H^+, Na^+, and Ca^{2+} on the layer surface are counterbalance charges of Bentonite [13].

In recent years, many papers have reported on the removal of heavy metal, dye, and other pollutants by using various types of Bentonite [13–16]. In addition, the ability of adsorption of many metals such as Cd, Zn, Fe, Hg, Cr, Cu, Mn, and Pb onto Bentonite has been well recognized [16–18].

The literature survey shows that Bentonite is one of the significant adsorbent to remove and to separate lead from solution, because it has high cation exchange capacity (90–120 meq/g), high elasticity and plasticity, low cost, easy handling, abundance as an adsorbent, and easy refining [19]. In the last two decades, the removal of lead from wastewater has been studied considerably [20]. The removal of lead from aqueous solution with Bentonite has been reported since 1993 [21]. After this mentioned time, various types of raw and modified Bentonite have been used as adsorbent to remove lead [22–26] (Table 1).

Bentonite has been modified by 8-hydroxy quinoline [27], sodium tetra borate [28], acid activated Bentonite (AAB) [29], sodium compounds [30], iron oxide and magnesium oxide [23], and

Table 1
Summary of Bentonite adsorbent to removal of lead

Adsorbent	Amount of adsorption (mg/g)	Reference
8-hydroxy quinoline-immobilized Bentonite	142.94	[27]
Sodium tetraborate-modified Kaolinite clay	42.92	[28]
MX-80 Bentonite	68.52	[25]
Acid activated (AAB) Bentonite	2.3175	[29]
Native Bentonite(NB)	8.11	[29]
Na-Bentonite	52.16	[30]
GMZ Bentonite	23.8	[26]
4-aminoantipyrine immobilized Bentonite	55.5	[18]
Raw Bentonite (RB)	16.7	[23]
Iron oxide-coated Bentonite (ICB)	22.2	[23]
Magnesium oxide-coated (MCB)	31.86	[23]
Raw Bentonite	79.36	This study
Bentonite modified with NH₄Cl	94.34	This study
Bentonite modified with NaCl	102.04	This study

4-aminoantipyrine [18] for removing lead. The best result of lead adsorption is related to 8-hydroxy quinoline-immobilized Bentonite with the adsorption capacity of 142.9 mg/g of lead [27].

Although these mentioned reports covered the subject well, Iranian Bentonite has not yet been studied very well for removing heavy metal (particularly for removing lead from aqueous solution). In this study, the main factors involved in the adsorption process and the determination of optimum conditions for reaching the best adsorption efficiencies were attained. The main purpose of this study is to investigate utilization of Iranian Bentonite (Isfahan area) to remove lead from aqueous solution. The adsorption isotherms models as Langmuir, Freundlich, Temkin, and Dubinin–Radushkevich (D–R) have been investigated for lead adsorption process into Iranian Bentonite.

2. Experimental

2.1. Material

A representative sample of Bentonite from Isfahan region in central of Iran was used without any chemical pretreatment and modification in the

Fig. 1. XRD pattern of raw Bentonite, NaCl–Bentonite, and NH_4Cl–Bentonite.

adsorption studies. The sample was ground and sieved by ASTM standard sieves to obtain the nominal particle size fractions of $-600+425$, $-425+300$, $-300+150$, $-150\,\mu m$ in diameter.

X-ray diffraction (XRD) and X-ray fluorescence (XRF) were used to determine the mineralogy of the sample and its elemental analysis. The XRD of the sample is shown in Fig. 1, and the elemental analysis of the sample is shown in Table 2. As shown in Table 2, the main mineral of sample contains montmorilonite. All chemical compounds were purchased from Merck and were used without further purification.

Table 2
Chemical analysis of raw Bentonite sample (XRF data)

Samples	SiO_2	Al_2O_3	MgO	Na_2O	Fe_2O_3	CaO	Cl	SO_3	K_2O
WT%	62.3	15.5	2.29	2.25	2.02	1.92	0.2	0.72	0.4

2.2. Physical measurements

XRD spectra and XRF were obtained using a Philips X-ray diffractometer 1,140 ($\alpha = 1.54$ A, 40 kV, 30 mA, calibrated with Si-standard) and a Philips X-ray diffractometer Xunique II (80 kV, 40 mA, calibrated with Si-standard), respectively. Infrared (IR) spectroscopy has been used for chemical functional groups. IR spectra from 4,000 to 400 cm^{-1} were recorded on a Shimadzu IR instrument, using KBr pellets. The specific surface area and microspores area were measured by Brunauer–Emmett–Teller method (nitrogen adsorption isotherm) [32]. The concentration of lead solution after adsorption was determined by use of atomic absorption spectrometry of unicam 939. Lead adsorption was calculated with respect to the amount of lead in the solution.

2.3. Experimental method

The lead adsorption experiments were carried out by using the batch equilibrium. All the adsorption experiments were conducted in a 250 mL glass reactor using a magnetic stirrer for mixing at ambient temperature. In this study, the influence of the parameters such as mass of Bentonite (from 10 to 50 g/L), particle size (from −150 to −600 μm), lead initial concentration (from 500 to 10,000 ppm), contact time (from 30 to 360 min), and stirring speed (from 400 to 700 rpm) in lead adsorption was investigated and finally, the optimized conditions were determined for maximizing lead adsorption. For investigating the effect of each parameter in each test, all parameters were kept constant unless a desirable one. Experiments were repeated with selecting and changing this desirable parameter. For investigating adsorption isotherms models (Langmuir, Freundlich, Temkin, and Dubinin–Radushkevich) a weighted Bentonite (1 g) was added to 100 mL of different concentration of lead solution ranging from 500 to 10,000 ppm. All of the solutions after each test were immediately subjected to filtration and then lead concentration in solution was determined by atomic absorption.

3. Results and discussions

3.1. Characterization of Bentonite

Fig. 1 shows XRD results for raw Bentonite, NaCl-Bentonite, and NH$_4$Cl-Bentonite. This mineral-ogical study revealed that the main constituents of the sample are Quartz, Andesine, Montmorillonite, Gypsum, and Halite. The diffraction peaks of raw Bentonite, NH$_4$Cl-Bentonite, and NaCl-Bentonite at range of 6°–7° 2θ relate to plane (0 0 1) which has been overlapped with illite diffraction peak. This Bentonite sample contains a low illite content. Andesine and Gypsum are the main impurities in these samples, which are obvious in the XRD pattern. Although the spectra of XRD of raw Bentonite and modified Bentonite demonstrate approximately the same peaks but this data reveal that the modification of Bentonite with NaCl and NH$_4$Cl were effective on the surface of Bentonite. In addition, it seems that the modification of Bentonite did not affect the crystal structure of Bentonite and there is no effective intercalation between layers of Bentonite. At last, the intensity of montmorilonite peak of modified Bentonite with NH$_4$Cl at plane (0 0 1) shows a reduction in comparison with raw Bentonite and NaCl-Bentonite. It indicates that the crystal degree of monmorilonite may be decreased by NH$_4$Cl and it would be the main clue of intensity peak decrease at plane (0 0 1). Table 2 displays the chemical analysis of the Bentonite sample from Isfahan area and that the amount of Na element to the amount of Ca ratio is 1.21. This ratio indicated that the type of Iranian Bentonite (from Isfahan area) is a mixed calcium and sodium Bentonite (calcium-sodium Bentonite).

The IR data of clays are usually used to predict their solid-state structures and characterization of atomic bonding. IR spectra of the raw Bentonite, NaCl–Bentonite, and NH$_4$Cl–Bentonite have been illustrated in Fig. 2. In addition, the main vibrational modes of IR spectra have been summarized in Table 3. IR spectra of the raw Bentonite, NaCl–Bentonite, and NH$_4$Cl–Bentonite show stretching bands at 3,630 and 3,629 cm^{-1}. Those indicate that O–H bond linkage of hydroxyl group which has an interaction with ions (Si–OH and Al–OH). The board-stretching band at 3,444 cm^{-1} for raw Bentonite concern to H–O–H starching band of water molecules within crystal structure of Bentonite, this board bond is due to hydrogen bonding between hydrogen and oxygen of different water molecules [27]. The H–O–H stretching bands of water molecules for NaCl–Bentonite and NH$_4$Cl–Bentonite are observed at 3,431 and 3,420 cm^{-1}, respectively. The decrease in waves' number of stretching vibration bands of H–O–H

Fig. 2. IR spectra of (a) raw Bentonite, (b) NaCl–Bentonite, and c) NH4Cl–Bentonite.

for modified Bentonite is related to presence of Na^+ and NH_4^+ ions between tetrahedral sheets and octahedral sheets. The NH_4^+ is more effective on vibrational data of H–O–H bond. The XRD data is revealed that Na^+ and NH_4^+ ions did not affect effectively crystal structure but these ions can destroy hydrogen-bonding interaction of water molecules in crystal structure of Bentonite, which it is observed by shift of stretching bands of H–O–H molecules in IR spectra.

The specific surface area for raw Bentonite, NaCl–Bentonite, and NH4Cl–Bentonite is 83, 115, and $104 \, m^2/g$, respectively. The microporous area for raw Bentonite, NaCl–Bentonite and NH4Cl–Bentonite is 21, 30, and $27 \, m^2/g$, respectively. This result is in

accordance with increase of lead adsorption onto modified Bentonite.

The bending vibration of H–O–H in water molecule in sample was observed at 1,649, 1,644, and $1,646 \, cm^{-1}$. The strong and broad band at $1040 \, cm^{-1}$ is related to stretching vibration in the Si–O–Si functional group in tetrahedral sheets of montmorillonite for raw and modified Bentonite [18]. The bending vibration bands at 469 and $468 \, cm^{-1}$ indicates to Si–O–Al and the bending vibrational data of Si–O–Si bonds are observed at 525 and $523 \, cm^{-1}$. The band at $693.61 \, cm^{-1}$ and near small shoulder (not assign in Fig. 2) could belong to the deformation and bending modes of the Si–O bond. The presence of quartz in

Table 3
The main vibrational modes of IR spectra

Assignment	Bentonite samples (cm^{-1})		
	Raw	NaCl	NH$_4$Cl
$\sqrt{}$ (X–O–H), X = Al, Mg	3,630	3,629	3,629
$\sqrt{}$ (H–O–H)	3,444	3,431	3,420
δ (H–O–H)	1,648	1,649	1,644
$\sqrt{}$ (Si–O)	1,040	1,040	1,040
δ (Al–Al–OH)	910	911	911
$\sqrt{}$ (Si–O–SiO$_2$)	706	796	796
δ (Al–O–Si)	525	525	523
δ (Si–O–Si)	469	468	468

this sample can be proved by IR with shoulder bonding at 796–793 cm^{-1} [30,31].

3.2. Adsorption characteristics

Investigation of the adsorption process onto Bentonite is important due to the application of this mineral as commercial natural adsorbents for controlling lead release. This investigation includes and covers characterization of Bentonite, optimum conditions of lead adsorption onto Bentonite, and study of adsorption isotherm models. These mentioned topics are reported and described in following section.

3.2.1. Effect of mass of Bentonite

In order to study the effect of mass of Bentonite on the removal of lead from solution, the mass of Bentonite has been varied from 1 to 5 g with constant concentration of lead (1,000 ppm) at temperature of 25℃, a stirring speed of 500 rpm, and a particle size of −150 μm. Fig. 3 presents the results of adsorption of lead with different Bentonite values. It is obvious that the adsorption percentage of lead is a function of Bentonite mass. On the other hand, the increasing of adsorbent material to liquid ratio has been caused an increase in the output of the percentages of adsorption.

The results on adsorption percentage of lead increase with increasing the mass of adsorbent up to 2 g with the adsorption of 100%. In addition, after that, the adsorption percentage is approximately constant. The improvement of adsorption values in high percentage of solid can be attributed to the fact that the amount of Bentonite available sites to each lead ions for adsorption increases with increasing mass of Bentonite in solution [24–26]. In the adsorption processes, mass of Bentonite is a significant
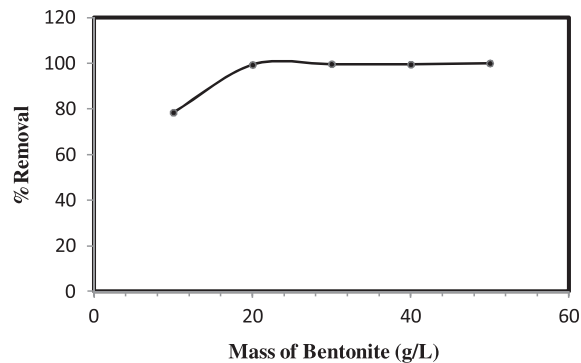

Fig. 3. Effect of mass of Bentonite on the adsorption of Pb (II) to Bentonite, pH: 3, C[Pb(II)]$_{initial}$: 1,000 ppm, T: 298 K, particle size: −150 μm, speed stirrer: 600 rpm, contact time: 30 min.

parameter because this factor determines the adsorption capacity of Bentonite for a given initial concentration of lead. The investigation of the effect of Bentonite mass on lead adsorption is shown in Fig. 3. In general, Bentonite without modification has relatively low lead adsorption (less than 20 mg/g) [23] but in this study, it has been observed that Isfahan Bentonite has a particular behavior for adsorption of lead because 2 g of this sample without any chemical and physical pretreatment could remove lead completely from solution with 1,000 ppm lead concentration. This property originates from amount and kind of effective sites and structure of Bentonite.

The adsorption percentage (α) and distribution coefficient (K_d) constant were calculated by following equation:

$$K_d = \frac{C_0 - C_{eq}}{C_0} \times V/m \tag{1}$$

$$\alpha = \frac{C_0 - C_{eq}}{C_0} \times 100 \tag{2}$$

where C_0 (mg/L) is initial lead concentration, C_{eq} (mg/L) is lead concentration in solution after adsorption process, V (L) is the volume of the solution, and m (g) is the mass of the Bentonite.

In Fig. 4 and it has been shown that the k_d value decreases with increasing Bentonite content from 1 g/100 mL to 50 g/100 mL. The increase of mass of Bentonite has occurred in a fixed volume, thereby it makes a competition among available sites on the Bentonite which causes the limitation of activity of available sites and therefore distribution coefficient constant was decreased with increasing of Bentonite content [24,32]. In the other word, when
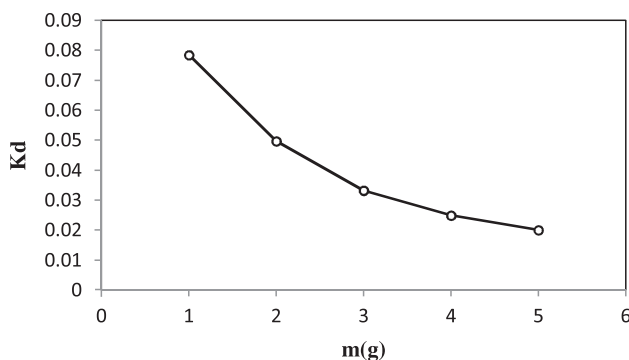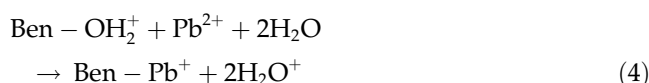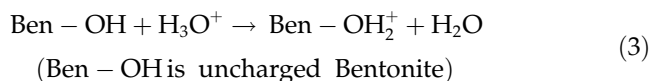
Fig. 4. Effect of mass of Bentonite on the value of K_d for adsorption of Pb to Bentonite, pH: 3, C[Pb(II)]$_{initial}$: 1,000 ppm, T: 298 K, particle size: $-150\,\mu$m, speed stirrer: 600 rpm, contact time: 30 min.

adsorption percentage value of lead is increased, the distribution coefficient (K_d) of lead adsorption onto Bentonite is decreased.

Lead atom interacts with oxygen of Bentonite as hard acid. Lead element has six electrons in the valance bond layer that electrons are in S and P orbitals therefore the Pb–O complex is stabilized by overlapping of P orbitals of oxygen atom and lead atom. With respect to this fact that Pb(II) species are a function of pH, at pH < 5 lead ions are observed in solution as lead free ions Pb(II) but at pH > 5 the predominating specie in solution is Pb(OH)$_n^m$ ($n = 1$–4 and $m = +1$ to -2). In this study, the adsorption of lead onto Iranian Bentonite has been done in acidic solution (3 pH) because industrial waste water is acidic solution (pH is around 3).

Mechanism of lead ion adsorption onto Bentonite is mainly inner-sphere or outer-sphere surface complexation and Ion exchange [25]. It seems these two mechanisms are participated in lead adsorption onto Bentonite in acidic solution. Ion exchange with hydronium (H$_3$O$^+$) of lead adsorption can be postulated as follows [25]:

$$Ben-OH + H_3O^+ \rightarrow Ben-OH_2^+ + H_2O$$

$$(Ben-OH \text{ is uncharged Bentonite})$$ (3)

$$Ben-OH_2^+ + Pb^{2+} + 2H_2O$$
$$\rightarrow Ben-Pb^+ + 2H_2O^+$$ (4)

3.2.2. Effect of contact time

The effects of contact time on the adsorption of Pb (II) onto Bentonite were investigated with using constant concentration of lead (1,000 ppm) and particle size of Bentonite-150 μm at ambient temperature. The results have been shown in Fig. 5. Different contact time with range from 30 to 360 min was studied for adsorption of Pb(II). The adsorption of lead into Bentonite increased rapidly at the initial contact time of 30 min. Therefore, 30 min contact time was chosen for all further studies. With the increase of contact time, the adsorption efficiencies were improved, especially in the periods of 30–120 min. When the adsorption time is 120 min, the adsorption efficiency reached to 84% at room temperature by using solid to liquid ratio of 10 g/L. When the contact time of adsorption reached above 120 min, there was no significant difference in the adsorption efficiencies. This equilibrium comes from this fact that the diffusion of lead from the surface sites to the interlayer of the solid is controlling the adsorption process [24]. The fast adsorption of Pb(II) on Bentonite indicates that Pb (II) adsorption is the main chemical adsorption [26].

It seems that Pb (II) ions at early stage quickly form complexes with negative permanent charge as silanol (Si–O$^-$) and aluminol (Al–O$^-$) groups on edges of Bentonite surface [17] and second other cations such as Na$^+$ or H$^+$ competes Pb(II) adsorption onto Bentonite.

3.2.3. Effect of particle size

In general, the particle size of Bentonite has an important influence on the amount of lead adsorption. The finer particle size has the greater geometric of external surface area and the greater degree of contact between lead ions and the particles of Bentonite. Table 4 shows that decreasing the particle size of Bentonite from -600 to $-150\,\mu$m could cause an increase in adsorption of lead ions onto Bentonite. These situations can attributed to the increasing
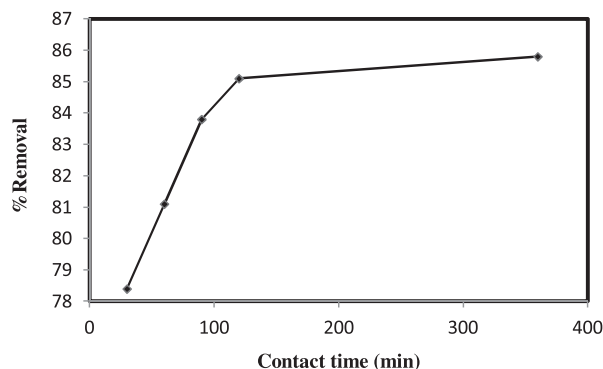

Fig. 5. Effect of contact time on the adsorption of Pb(II) to Bentonite, pH: 3, m/V: 10 g/L C[Pb(II)]$_{initial}$: 1,000 ppm, T: 298 K, particle size: -150μ, speed stirrer: 600 rpm.

Table 4
Effect of particle size on the adsorption of Pb(II) to Bentonite, Ph: 3, m/V: 10 g/L, C [Pb(II)]$_{initial}$: 1,000 ppm, T: 298 K, stirring speed: 600 rpm, contact time: 30 min

Particle size (μm)	Pb remain ppm	% remove
−150	216	78.4
−300 + 150	245	75.5
−425 + 300	382	61.8
−600 + 425	506	49.4

contact surface of the Bentonite particle as the particle size decreases.

On the other hand, activity of functional groups for ions adsorption has been increased with decreasing of particle size of Bentonite. When particle size was −600 + 425 μm, the adsorption of lead was reached the lowest value at 49.4%. According to these results, Bentonite with particle size of −150 μm is appropriate for maximum adsorption of lead. Then Bentonite with particle size of −150 μm was chosen for all further studies.

3.2.4. Effect of stirring speed

Adsorption experiments were conducted at 25°C to determine the effect of the stirring speed by using solid to liquid ratio 0.01. The lead adsorption onto Bentonite at 30 min was 60.0, 61.9, and 78.4%, at 400, 500, and 600 rpm stirring speed, respectively. The results showed that the adsorption rate increased by increasing stirring speed up to 600 rpm and over that amount, the rate of agitation did not influence the lead adsorption, as shown in Fig. 6. In general for adsorption, the stirring of solution would cause to a decrease of the boundary layer and the resistance of transition of lead ions [10]. By reaching beyond the stirring speed 700 rpm, the stirring speed would not
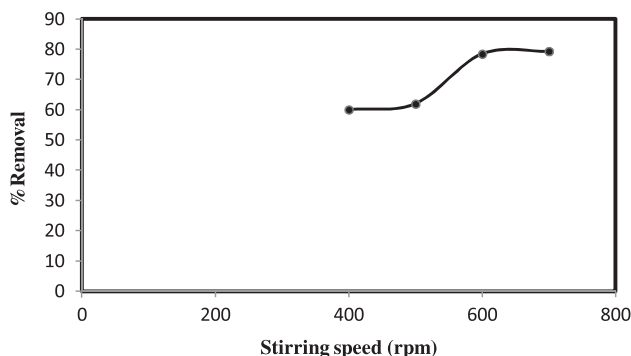
affect on the uptake of lead ions. On the other hand, it indicated that over stirring speed 600 rpm, there was an adequate suspension of the solid particles as well as adequate distribution of lead ions in the solution that it originates the increasing stirring speed over 700 rpm could not be effective on difference lead concentration on the surface of Bentonite and lead concentration of the bulk solution; hence an intermediate rate of 600 rpm was used in all experiments to assure the independency of this variable.

3.2.5. Effect of initial concentration

On set condition of mass of Bentonite to liquid (m/V = 50 g/L) and particle size of −150 μm, the adsorption of lead into Bentonite has been studied at different initial concentration of lead range from 500 to 10,000 ppm. Data on the adsorption of lead are shown in Fig. 7. The removal percentage of lead was decreased with increasing in initial lead concentration from 500 to 10,000 ppm. Of course, amount of lead adsorbed onto one unit of Bentonite has been increased in initial lead concentration from 500 to 10,000 ppm.

3.3. Adsorption isotherms

A number of experiments were performed to evaluate of the Langmuir, Freundlich, Temkin, and Dubinin–Radushkevich(D–R) adsorption isotherms models at initial various lead concentrations as 800, 1,000, 2,000, 5,000, and 10,000 ppm.

3.3.1. Langmuir isotherm

The linear form of the Langmuir isotherm model is assuming the adsorption metal ions homogeneously
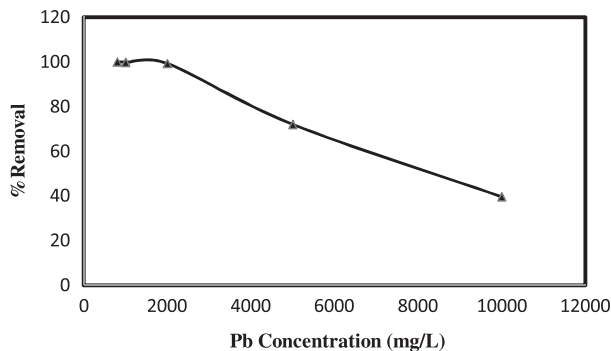

Fig. 6. Effect of speed stirrer on the adsorption of Pb(II) to Bentonite, pH: 3, m/V: 10 g/L C[Pb(II)]$_{initial}$: 1,000 ppm, T: 298 K, particle size: −150 μm, contact time: 30 min.

Fig. 7. Effect of Pb(II) ion concentration on the adsorption of Pb(II) to Bentonite, pH: 3, m/V: 50 g/L, T: 298 K, particle size: −150 μm, stirring speed: 600 rpm, contact time: 30 min.

(uniform) onto the surface with a finite number of adsorption sites, by a monolayer adsorption process. Of course, this model assumes adsorptive molecules interact with active sites on the surface Bentonite that they have identical energy. The equation of Langmuir isotherm model is as follows:

$$\frac{C_e}{q_e} = \frac{1}{b\,Q_0} + \frac{C_e}{Q_0} \qquad (5)$$

where q_e (mg/g) is the amount of adsorption cadmium per unit weight of Bentonite and and C_e (mg/L) is cadmium concentration in solution at equilibrium (after adsorption). The b is the Langmuir isotherm constants that related to the free energy of adsorption. On the other hand, b is related to binding energy of active site of Bentonite and Q_0 is adsorption capacity maximum in monolayer adsorption [33–35].

Fig. 8 shows the plots of linear form of Langmuir of raw Bentonite, NaCl–Bentonite, and NH4Cl–Bentonite with correlation coefficient (r^2) more than 0.995 and straight lines. These lines are approximately parallel together with slopes between 0.009–0.012.

The maximum adsorption capacity according to Langmuir monolayer adsorption model for raw Bentonite, NaCl–Bentonite, and NH4Cl–Bentonite are 79.34, 102.04, and 94.33 mg/g, respectively. These values of adsorption capacity for raw Bentonite and modified Bentonite in comparison with other reports are considerable [36]. The equilibrium constant values (b) that related to binding energy of active site of Bentonite with ion metals for raw Bentonite, NaCl–Bentonite, and NH4Cl–Bentonite are 0.0292 L/mg, 0.0044, and 0.0043, respectively. Also the results show that maximum adsorption capacity (Q_0) and equilib-

rium constant value (*b*) values increase in Bentonite modification.

The Langmuir isotherm model can be displayed in terms of a dimensionless constant that called separation factor R_L (also called equilibrium parameter) which is presented by this equation [37–39].

$$R_L = \frac{1}{1 + b\,C_0} \qquad (6)$$

where C_0 (mg/L) is the initial cadmium concentration and b (L/mg) is the Langmuir constant related to the energy of adsorption. Fig. 9 is showing the plots of separation factor (R_L) vs. initial concentrations of lead between 100 and 1,500 ppm for the range of raw Bentonite, NaCl–Bentonite, and NH4Cl–Bentonite are 0.0056–0.9607, 0.0526–0.5594, and 0.0528–0.5259, respectively. These data are indicating that lead adsorption into Bentonite for lead various concentrations is favorable and reversible because $0 < R_L < 1$.

Table 6 and Fig. 9 display the removal of lead from solution by modified Bentonite with more favorite than raw Bentonite. The result of Fig. 9 show R_L at high lead concentration the separation factor for modified Bentonite is better than raw Bentonite but at low lead concentration separation factor for raw Bentonite is better than modified Bentonite.

Along with correlation coefficient (r^2), standard deviation (SD) is necessary to evaluate the data of adsorption set to confirm the best fit of isotherm model for the adsorption system which is presented as follows [40,41]:

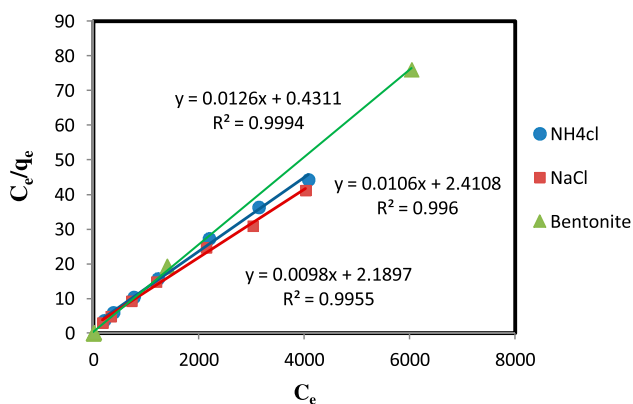$$SD = \sqrt{\frac{\sum \left[(q_{t,exp} - q_{t,cal})/q_{t,exp} \right]^2}{(n-1)}} \qquad (7)$$

Fig. 8. Langmuir isotherms for Pb(II) adsorption onto crude Bentonite, NaCl-Bentonite and NH4Cl–Bentonite, pH: 3, m/V: 50 g/L, T: 298 K, particle size: −150 μm, stirring speed: 600 rpm, contact time: 30 min.
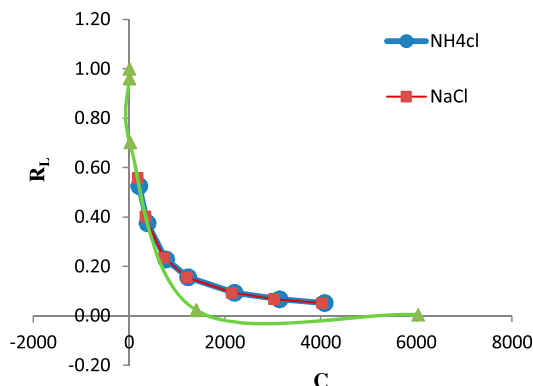

Fig. 9. Plot of separation factor vs. initial concentrations of lead between 100 and 1,500 ppm for the range of raw Bentonite, NaCl–Bentonite, and NH4Cl–Bentonite.

This equation shows SD of adsorption process test. It basically explains the sum of the squares of the differences between the experimental data of adsorption ($q_{t, exp}$) and data obtained by calculating from adsorption models ($q_{t, cal}$), with each squared difference divided by the corresponding data obtained by calculating from models. In this equation, n is the number of data points (number of experimental data). If obtained data from this model are similar to experimental data, SD will be a small number and data approach to zero but if SD gains a higher value (approaches to unit), the deviation of data from the model would be higher. The values of SD for raw and modified Bentonite for all models are less than 0.2 (unless for raw Bentonite for Langmuir model).

In addition, Table 5 summarizes Langmuir model parameters such as maximum capacity (Q_m), Langmuir constant (b), and correlation coefficient (R^2) related to adsorption lead into clay. This data shows that maximum capacity of Iranian bentonie (from Isfahan area) according to Langmuir model without any modification is better than the one found by other researches [21,23–25,29,30].

3.3.2. Freundlich isotherm

The Freundlich isotherm models describe the non-ideal, multilayer adsorption, and adsorption on heterogeneous surfaces, which is assumed that the adsorption process is reversible. The Eq. (8) represents Freundlich isotherm model [38].

$$\log q_e = \log K_F + 1/n \log C_e \tag{8}$$

where K_F ($mg^{1-1/n} L^{1/n} g^{-1}$) and n (g/L) are Freundlich constants which represent adsorption capacity of the Bentonite and adsorption intensity (or surface heterogeneity) of the adsorbent, respectively.

Table 5
Langmuir isotherm constants for lead adsorption onto different adsorbents

No	Material	Q_m (mg/g)	b (L/mg)	R^2	Ref
1	Bentonite	52.63	63.33		[21]
2	MX-80 Bentonite	68.5	0.021	0.945	[25]
3	Tunisian smectite-rich clay	25	0.99	0.99	[24]
4	Bentonite	8.28	0.143	0.996	[29]
5	Na-Bentonite	47.81	0.097	0.995	[30]
6	Raw-Bentonite	16.7	1.3	0.986	[23]
7	GMZ (GaomiaoziCounty) Bentonite	23.8	0.48	0.999	[26]
8	The Iranian Bentonite (Isfahan area)	79.36	0.029	0.999	This study

Table 6
Langmuir, Freundlich, Temkin, and Dubinin–Radushkevich isotherm constants for lead adsorption

Model	Parameter	Crude Bentonite	NaCl–Bentonite	NH$_4$Cl–Bentonite
Langmuir	q_m (mg/g)	79.365079	102.040816	94.339623
	R^2	0.9994	0.9955	0.996
	SD	0.469518	0.097096	0.076777
	R_L	0.0056–0.9607	0.0526–0.5594	0.0528–0.5259
	b	0.029228	0.004475	0.004397
Freundlich	K_F ($mg^{1-1/n} L^{1/n} g^{-1}$)	19.13375	21.35010	23.31310
	n (g/L)	5.83431	5.64334	5.74383
	R^2	0.98970	0.99510	0.99430
	SD	0.01494	0.01971	0.02060
Temkin	b (J/mol)	9.77280	15.29700	23.44200
	A (L/mg)	0.27370	0.00240	0.00155
	R^2	0.92850	0.99030	0.99070
Dubinin–Radushkevich	β	2.00E-04	6.00E-06	7.00E-06
	E (kJ)	0.05	0.288675	0.2672612
	R^2	0.9394	0.923	0.9509
	SD	0.16110	0.03000	0.02493

This equation indicates that at the first of adsorption process, the stronger binding sites are occupied and subsequently the decrease of adsorption energy is observed as exponential reduction [34,39,42].

Fig. 10 shows the plots of linear form of Freundlich for raw Bentonite, NaCl–Bentonite, and NH$_4$Cl–Bentonite with correlation coefficient (R^2) more than 0.980. Adsorption capacity of the Bentonite in Freundlich isotherm model for NH$_4$Cl–Bentonite (23.3 mg/g) is better than raw Bentonite (19.13 mg/g) and NaCl–Bentonite (21.35 mg/g).

The Freundlich isotherm parameter ($1/n$) determinates from plot of $\ln q$ against $\ln C_e$. This value coefficient indicates to the adsorption intensity of lead ions on the clay. The slope of linear plots in Fig. 8 shows that n for raw Bentonite, NaCl–Bentonite, and NH$_4$Cl–Bentonite are 5.83, 5.64, and 5.74, respectively. According to literature survey, the adsorption process is favored in the case of $1 < n < 10$. Therefore, the data adsorption of lead is fitted to Freundlich completely, that is, the adsorption intensity (n) for raw Bentonite is approximately as same as modified Bentonite. Of course, Freundlich model paremeter (n, SD, R^2) for lead adsorptuion onto modified Bentonite is better than raw Bentonite.

3.3.3. Temkin isotherm

The linear form of the Temkin isotherm is presented as follows Eq. (9).

The obtained adsorption data were investigated by Temkin adsorption isotherm model according to Eq. (9) [27,43].

$$q_e = RT/b \, \mathrm{Ln}\, A + RT/b \, \mathrm{Ln} C_e \qquad (9)$$

where b and A are Temkin isotherm constants, b is a constant that related to the heat of adsorption (J/mol).

In this equation, R is the gas constant (8.314 J/mol K) and T is the absolute temperature. The q_e (mg/g) is the equilibrium concentration of cadmium adsorbed into Bentonite. The Eq. (5) shows amount of adsorption in the layer is related to logarithm of equilibrium concentration of adsorbate in solution that A and b are determined from the intercept and slope of the linear plots of q_e vs. $\ln C_e$. In this model, it was assumed that the binding energies of adsorbent–adsorbate interactions are uniformly distributed which caused the decrease linearly of heat of adsorption. On the other hand, Temkin model has modified Langmuir model by applying the effect of temperature in adsorption processes [27,43].

The Temkin isotherm plots for raw Bentonite, NaCl–Bentonite, and NH$_4$Cl–Bentonite are displayed in Fig. 11. The modified Bentonite by NaCl and NH$_4$Cl have correlation coefficient (R^2) 0.995 and 0.994, respectively. These values are higher than correlation coefficient (R^2) of raw Bentonite.

The values of b constants for raw Bentonite, NaCl–Bentonite, and NH$_4$Cl–Bentonite are 0.009, 0.015, and 0.023 kJ/mol, respectively, that indicate to the presence of weak interaction between active sites of Bentonite and lead ions. It means a physical adsorption process.

3.3.4. Dubinin–Radushkevich (D–R) isotherm

The empirical's Dubinin–Radushkevich model isotherm was introduced in 1947, which was assumed for homogenous surface adsorption [44]. This model can be distinguished between physical and chemical adsorption of metal ions. The model is presented by Eq. (10):

$$\mathrm{Ln}\, q = \mathrm{Ln}\, q_{max} - \beta R^2 T^2 \mathrm{Ln}^2(1 + 1/C) \qquad (10)$$
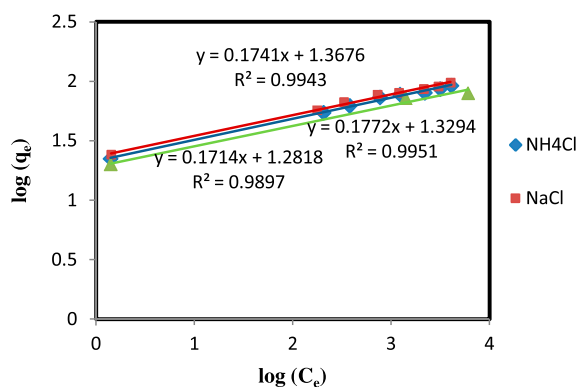

Fig. 10. Freundlich isotherms for Pb(II) adsorption onto crude Bentonite, NaCl–Bentonite, and NH$_4$Cl–Bentonite, pH: 3, m/V: 50 g/L, T: 298 K, particle size: $-150\,\mu$m, stirring speed: 600 rpm, contact time: 30 min.
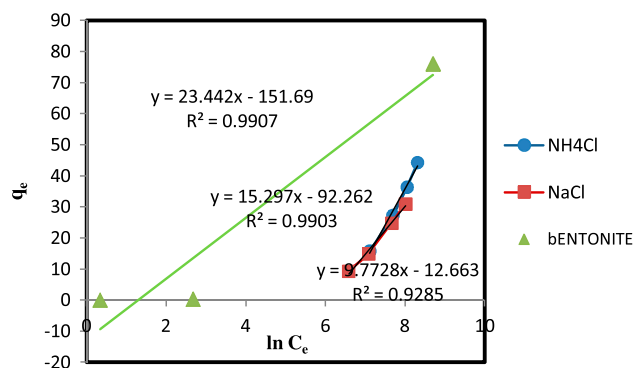

Fig. 11. Temkin isotherms for Pb(II) adsorption onto crude Bentonite, NaCl–Bentonite, and NH$_4$Cl–Bentonite, pH: 3, m/V: 50 g/L, T: 298 K, particle size: $-150\,\mu$m, stirring speed: 600 rpm, contact time: 30 min.

where R is the gas constant (8.314 J/molK), T is the absolute temperature, q_m is capacity maximum of adsorption (mg/g), and β is a constant related to adsorption energy (mol²/KJ²). According to Eq. (11) with using β, free energy per molecule of adsorbate (E) can be calculated [45].

$$E = \frac{1}{\sqrt{2\beta}} \tag{11}$$

If adsorption energy is $Ea < 8$ kJ/mol, the adsorption would be done physically. For chemical absorption or ion exchange, the adsorption energy would be $8 < Ea < 16$ kJ/mol and while for the values of $Ea > 16$ kJ/mol the particle diffusion is controlling the process [46,47].

The plots of linear form of $Ln\,q_e$ vs. $Ln^2(1 + c^{-1})$ with correlation coefficient (r^2) between 0.92–0.95 for raw Bentonite and modified Bentonite have been shown in Fig. 12. The parameters q_m and B are calculated from the intercepts and slopes, respectively. According to Table 6 adsorption free energy (E) is 0.05 kJ for raw Bentonite which is increased to 0.28 and 0.26 kJ for NaCl–Bentonite and NH$_4$Cl–Bentonite, respectively, that is, the adsorption of lead by Bentonite is a physical process.

3.3.5. Evaluation of adsorption isotherm models of lead onto Bentonite

In spite of the close similarity of these correlation coefficients (r^2) of plot of models, it could be concluded that the adsorption of lead into Bentonite could be better described by Langmuir model rather than by Freundlich, Temkin, and Dubinin–Radushkevich (D–R) models. The empirical constants of Freundlich and Langmuir, Temkin, and Dubinin–Radushkevich (D–R) models are observed in Table 6. Of course, modification
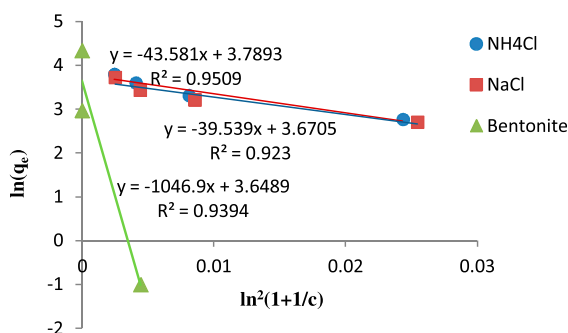
of bentoniute has been caused to improve correlation coefficients (r^2) of plot of Freundlich, Langmuir, Temkin, and Dubinin–Radushkevich (D–R) models more than 0.990 which indicates NaCl and NH$_4$Cl compounds have complexity treatment onto Bentonite. The maximum adsorption capacity of Bentonite in monolayer adsorption process (Langmuir isotherm model) is 79 mg/g for raw Bentonite that the modification of Bentonite has been caused maximum adsorption capacity of Bentonite to higher value of 102 and 94 mg/g for NaCl–Bentonite and NH$_4$Cl–Bentonite, respectively. This result in comparison with other reports of lead adsorption onto Bentonite is considerable [23,24].

4. Conclusions

This contribution has shown that Iranian Bentonite from Isfahan area is suitable for acting as a filter to separate lead ions from aqueous solution by adsorption process. The results indicated that the optimum condition is achieved at the pH value of 3, particle size $-150\,\mu$m, solid to liquid ratio of 0.1 g/L, contact time of 120 min, and stirrer speed 600 rpm for reaching maximum lead adsorption on 1 g Bentonite at room temperature with initial concentration of lead 1,000 ppm. The removal efficiency of Bentonite increased with arising of mass of Bentonite. Thus percentage of adsorbed lead from lead aqueous solution (1,000 ppm) by 2 g raw Iranian Bentonite (from Isfahan area) is 100%.

According to the adsorption isotherms models, Langmuir displays the best model to describe adsorption of lead into raw Bentonite and modified Bentonite. The modification of Bentonite causes to enhance the efficiency of lead adsorption. The constants of Temkin and Dubinin–Radushkevich (D–R) models show the physical adsorption of lead by raw Bentonite and modified.

Fig. 12. Dubinin–Radushkevich isotherms for Pb(II) adsorption onto crude Bentonite, NaCl–Bentonite, and NH$_4$Cl–Bentonite, pH: 3, m/V: 50 g/L, T: 298 K, particle size: $-150\,\mu$m, stirring speed: 600 rpm, contact time: 30 min.

References

[1] C. Ake, K. Mayura, H. Huebner, G.R. Bratton, T.D. Phillips, Development of porous clay-based composites for the sorption of lead from water, Toxicol. Environ. Health Part A 63 (2001) 459–475.

[2] K.K. Chatterjee, Uses of industrial minerals, rocks, and freshwater, Nova Science, New York, 2009.

[3] S. Tunali, T. Akar, A.S. Ozcan, I. Kiran, A. Ozcan, Equilibrium and kinetics of biosorption of lead(II) from aqueous solutions by Cephalosporiumaphidicola, Sep. Purif. Technol. 47 (2006) 105–112.

[4] N. Das, R.K. Jana, Adsorption of some bivalent heavy metal ions from aqueous solutions by manganese nodule leached residues, Colloid Interface Sci. 293 (2005) 254–262.

[5] A. Krobba, D. Nibou, S. Amokrane, H. Mekatel, Adsorption of copper (II) onto molecular sieves NaY, Desalin. Water Treat. 37 (2012) 31–37.

[6] C. Morales Futalana, C. Chuan Kanb, M. Lourdes Dalidac, K. Jung Hsienb, C. Pascuad, M. WeiWanb, Comparative and competitive adsorption of copper, lead, and nickel using chitosan immobilized on Bentonite, Carbohydr. Polym. 83 (2011) 528–536.

[7] K. Kadirvelu, K. Thamaraiselvi, C. Namasivayam, Removal of heavy metals from industrial wastewaters by adsorption onto activated carbon prepared from an agricultural solid waste, Bioresour. Technol. 76 (2001) 63–65.

[8] Y. Feng, J.L. Gong, G.M. Zeng, Q.Y. Niua, H.Y. Zhang, C.G. Niu, J.H. Deng, M. Yan, Adsorption of Cd (II) and Zn (II) from aqueous solutions using magnetic hydroxyapatite nanoparticles as adsorbents, Chem. Eng. J. 162 (2010) 487–494.

[9] D. Nibou, H. Mekatela, S. Amokrane, M. Barkat, M. Trari, Adsorption of Zn^{2+} ions onto NaA and NaX zeolites: Kinetic, equilibrium and thermodynamic studies, J. Hazard. Mater. 173 (2010) 637–646.

[10] V.J. Inglezakis, M.A. Stylianou, D. Gkantzou, M.D. Loizidou, Removal of Pb(II) from aqueous solutions by using clinoptilolite and Bentonite as adsorbents, Desalination 210 (2007) 248–256.

[11] G.B. Krishna, S.G. Susmita, Kaolinite and montmorillonite as adsorbents for Fe(III), Co(II) and Ni(II) in aqueous medium, Appl. Clay Sci. 41 (2008) 1–9.

[12] T. Motsi, N.A. Rowson, M.J.H. Simmons, Adsorption of heavy metals from acid mine drainage by natural zeolite, Int. J. Miner. Process. 92 (2009) 42–48.

[13] Q. Li, Y. Su, Q.Y. Yue, B.Y. Gao, Adsorption of acid dyes onto Bentonite modified with polycations: Kinetics study and process design to minimize the contact time, Appl. Clay Sci. 53 (2011) 760–765.

[14] S. Babel, T.A. Kurniawan, Low-cost adsorbents for heavy metals uptake from contaminated water: A review, J. Hazard. Mater. 97 (2003) 219–243.

[15] Q. Yue, Q. Li, B. Gao, Y. Wang, Kinetics of adsorption of disperse dyes by polyepicholorohydrin-dimethylamine cationic polymer/Bentonite, Sep. Purif. Technol. 54 (2007) 279–290.

[16] R. Koswojo, R.P. Utomo, Y. Ju, A. Ayucitra, F.E. Soetaredjo, J. Sunarso, S. Ismadji, Acid Green 25 removal from wastewater by organo-Bentonite from Pacitan, Appl. Clay Sci. 48 (2010) 81–86.

[17] M.G.A. Vieiraa, A.F.A. Netoa, M.L. Gimenesb, M.G.C. da Silva, Removal of nickel on Bofe Bentonite calcined clay in porous bed, J. Hazard. Mater. 176 (2010) 109–118.

[18] Q. Wang, X. Chang, D. Li, Z. Hu, R. Li, Q. He, Adsorption of chromium(III), mercury(II) and lead(II) ions onto 4-aminoantipyrine immobilized Bentonite, J. Hazard. Mater. 186 (2011) 1076–1081.

[19] F. Bergaya, B.K.G. Theng, G. Lagaly, Handbook of Clay Science, Developments in Clay Science, vol. 1, Elsevier, publisher Newnes, Oxford, 2006 (Chapter11).

[20] H. Chen, A. Wang, Kinetic and isothermal studies of lead ion adsorption onto palygorskite clay, Colloid Interface Sci. 307 (2007) 309–316.

[21] R. Naseem, S.S. Tahir, Removal of Pb(II) from aqueous/acid solution by using Bentonite as adsorbent, Water Res. 35(16) (2001) 3982–3986.

[22] S.A. Al-Jlil, F.D. Alsewailem, Saudi Arabian clays for lead removal in wastewater, Appl. Clay Sci. 42 (2009) 671–674.

[23] E. Eren, Removal of lead ions by Unye (Turkey) Bentonite in iron and magnesium oxide-coated forms, J. Hazard. Mater. 165 (2009) 63–70.

[24] I. Chaari, E. Fakhfakh, S. Chakroun, J. Bouzid, N. Boujelben, M. Feki, F. Rocha, F. Jamoussi, Lead removal from aqueous solutions by a Tunisian smectitic clay, J. Hazard. Mater. 156 (2008) 545–551.

[25] D. Xu, X.L. Tan, C.L. Chen, X.K. Wang, Adsorption of Pb(II) from aqueous solution to MX-80 Bentonite: Effect of pH, ionic strength, foreign ions and temperature, Appl. Clay Sci. 41 (2008) 37–46.

[26] S. Wang, Y. Dong, M. He, L. Chen, X. Yu, Characterization of GMZ Bentonite and its application in the adsorption of Pb(II) fromaqueous solutions, Appl. Clay Sci. 43 (2009) 164–171.

[27] A.S. Ozcan, O. Gök, A. Ozcan, Adsorption of lead(II) ions onto 8 hydroxy quinoline-immobilized Bentonite, J. Hazard. Mater. 161 (2009) 499–509.

[28] E.I. Unuabonah, K.O. Adebowale, B.I. Olu-Owolabi, L.Z. Yang, L.X. Kong, Adsorption of Pb (II) and Cd (II) from aqueous solutions onto sodium tetraborate-modified Kaolinite clay: Equilibrium and thermodynamic studies, Hydrometallurgy 93 (2008) 1–9.

[29] A.R. Kul, H. Koyuncu, Adsorption of Pb(II) ions from aqueous solution by native and activated Bentonite: Kinetic, equilibrium and thermodynamic study, J. Hazard. Mater. 179 (2010) 332–339.

[30] S. Yang, D. Zhao, H. Zhang, S. Lu, L. Chen, X. Yu, Impact of environmental conditions on the sorption behavior of Pb(II) in Na-Bentonite suspensions, J. Hazard. Mater. 183 (2010) 632–640.

[31] M. Klinkenberg, R. Dohrmann, S. Kaufhold, H. Stanjek, A new method for identifying Wyoming Bentonite by ATR-FTIR, Appl. Clay Sci. 33 (2004) 195–206.

[32] S. Kaufhold, R. Dohrmann, M. Klinkenberg, S. Siegesmund, K. Ufer, N2-BET specific surface area of Bentonites, Colloid Interface Sci. 349 (2010) 275–282.

[33] G.Q. Tan, D. Xiao, Adsorption of cadmium ion from aqueous solution by ground wheat stems, J. Hazard. Mater. 164 (2009) 1359–1363.

[34] K.Y. Foo, B.H. Hameed, Insights into the modeling of adsorption isotherm systems, Chem. Eng. 156 (2010) 2–10.

[35] P. Chingombe, B. Saha, R.J. Wakeman, Sorption of atrazine on conventional and surface modified activated carbons, Colloid Interface Sci. 302 (2006) 408–416.

[36] A. Mockovciaková, Z. Orolínová, J. Skvarla, Enhancement of the Bentonite sorption properties, J. Hazard. Mater. 180 (2010) 274–281.

[37] M. Ozacar, I.A. Sengil, Adsorption of metal complex dyes from aqueous solutions by pine sawdust, Bioresour. Technol. 96 (2005) 791–795.

[38] G. Crini, H.N. Peindy, F. Gimbert, C. Robert, Removal of C.I. basic green 4, (malachite green) from aqueous solutions by adsorption using cyclodextrin-based adsorbent: Kinetic and equilibrium studies, Sep. Purif. Technol. 53 (2007) 97–110.

[39] A.E. Ofomaja, Y.S. Ho, Equilibrium sorption of anionic dye from aqueous solution by palm kernel fibre as sorbent, Dyes Pigm. 74 (2007) 60–66.

[40] E. Bulut, M. Ozacar, I.A. Sengil, Adsorption of malachite green onto Bentonite: Equilibrium and kinetic studies and process design, Microporous Mesoporous Mater. 115 (2008) 234–246.

[41] M. Ozacar, Contact time optimization of two stage batch adsorber design using second-order kinetic model for the adsorption of phosphate onto alunite, J. Hazard. Mater. 137 (2006) 218–225.

[42] J. Zeldowitsch, Adsorption site energy distribution, Acta Phys. Chim. URSS 1 (1934) 961–973.

[43] I.D. Mall, V.C. Srivastava, N.K. Agarwall, I.M. Mishra, Removal of Congo Red from aqueous solution by bagasse fly ash and activated carbon: Kinetic study and equilibrium isotherm analysis, Chemosphere 61 (2005) 492–501.

[44] J.P. Hobson, Physical adsorption isotherms extending from ultra-high vacuum to vapor pressure, Phys. Chem. 73 (1969) 2720–2727.

[45] M. Dogan, M. Alkan, O. Demirbas, Y. Ozdemir, C. Ozmetin, Adsorption kinetics of maxilon blue GRL onto sepiolite from aqueous solution, Chem. Eng. 124 (2006) 89–101.

[46] A. Ozcan, E.M. Oncu, A.S. Ozcan, Kinetic, isotherm and thermodynamic studies of adsorption of Acid Blue 193 from aqueous solution onto natural sepiolite, Colloids Surf., A 277 (2006) 90–97.

[47] E. Bulut, M. Ozacar, I.A. Sengil, Equilibrium and kinetic data and process design for adsorption of Congo Red onto Bentonite, J. Hazard. Mater. 154(1–3) (2008) 613–622.